Chinese Chemical Letters 34 (2023) 108195

Contents lists available at ScienceDirect

Chinese Chemical Letters

journal homepage: www.elsevier.com/locate/cclet

Double-cavity *nor-seco*-cucurbit[10]uril-based supramolecular assembly for selective detection and removal of trinitrophenol ☆

Ran Cen[1], Ming Liu[1], Jiao He, Dingwu Pan, Lixia Chen, Ying Huang, Zhu Tao, Xin Xiao*

Key Laboratory of Macrocyclic and Supramolecular Chemistry of Guizhou Province, School of Chemistry and Chemical Engineering, Guizhou University, Guiyang 550025, China

ARTICLE INFO

Article history:
Received 16 November 2022
Revised 26 January 2023
Accepted 5 February 2023
Available online 25 February 2023

Keywords:
Nor-seco-cucurbit[10]uril
8-Hydroxyquinoline
Supramolecular assembly
2,4,6-Trinitrophenol
Removal
Detection

ABSTRACT

The effective removal and selective detection of explosive and toxic pollutant trinitrophenol (TNP) is an attractive but challenging field. Herein, a double-cavity *nor-seco*-cucurbit[10]uril (*ns*-Q[10])-based supramolecular assembly 8-HQ@*ns*-Q[10] was fabricated and its structure was characterized by X-ray single crystal diffraction. In this assembly, the stoichiometric ratio of *ns*-Q[10] and 8-hydroxyquinoline (8-HQ) is 1:2, which is also attributed to the special double-cavity structure of *ns*-Q[10]. The luminescence sensing experiments showed that 8-HQ@*ns*-Q[10] can be used as a good fluorescence-enhanced sensing material (enhanced 27-fold) for the rapid detection of explosives and the aqueous contaminant TNP, with a limit of detection (LOD) of 2.07×10^{-5} mol/L, without interference from other phenolic compounds. Furthermore, TNP can be efficiently removed in the presence of assembly 8-HQ@*ns*-Q[10], and the removal efficiency is more than 89%. Therefore, the supramolecular assembly 8-HQ@*ns*-Q[10], as a fluorescence-enhanced luminescence sensor and adsorption material, has rich research value and potential application prospect when applied to the detection and removal of TNP in aqueous environment.

The nitroaromatic compound, 2,4,6-trinitrophenol (TNP), commonly known as picric acid, is not only a dangerous component of explosives, but also a contaminant in water and soil that can cause dangerous damage to internal organs and the nervous system [1]. Since TNP is an explosive and toxic pollutant, it is of great importance in both national security and environmental protection [2]. Therefore, the efficient identification and removal of TNP is very attractive and important for scientists. Despite the selectivity and accuracy of current explosives detection methods, including modern analytical techniques (colorimetric immunoassay [3], surface-enhanced raman spectroscopy [4], and ion mobility spectrometry [5]), they also suffer from high operating costs, portability issues during field use, and the need for frequent calibration. Therefore, the detection of explosive compounds or their precursors in a non-destructive manner is of considerable importance in today's security environment. In contrast, fluorescence detection methods have attracted increasing attention due to their cost-effectiveness, high sensitivity and relatively easy operation [6–10]. Although there are known reports for the detection of TNP explosives, the challenges remain with their rapidity and high sensitivity. Among the different materials that can be used as fluorescent sensors, organic frameworks are considered to be promising materials, metal-organic frameworks (MOFs) [11–13], polymers [14–16], and hybrid materials [17,18] have been reported for this purpose, which typically gradually change the fluorescence intensity of the sensor by adding analytes. The method is simple and sensitive, and can meet the requirements of rapid detection and high sensitivity of pollutants.

The study of nitroaromatic compounds using organic frameworks and supramolecular chemistry strategy has long been the focus of scientists' attention. Aggarwal reported a fluorescent Zr-NDI based MOF for the selective detection of trinitrophenol (TNP) in water. The limit of detection of TNP is as low as 8.1 ppm and the quenching efficiency is 95% [19]. Morsali designed a dual-responsive reproducible luminescent 2D-MOF for nitroaromatic sensing *via* targeted modulation of active interaction sites [20]. Zhao constructed a series of fluorescent heteroporous covalent organic frameworks and realized their application in the spectroscopic and visual detection of TNP with high selectivity and high sensitivity. The heteropore COFs exhibit spectroscopic and color changes to TNP with extremely high selectivity and sensitivity, which makes them excellent macroscopic chemosensors for the selective detection of TNP [21]. However, among the fluorescent

☆ Dedication to Prof. Lixin Dai on the Occasion of His Centenary Birthday.

* Corresponding author.
E-mail address: xxiao@gzu.edu.cn (X. Xiao).

[1] These authors contributed equally to this work.

https://doi.org/10.1016/j.cclet.2023.108195
1001-8417/

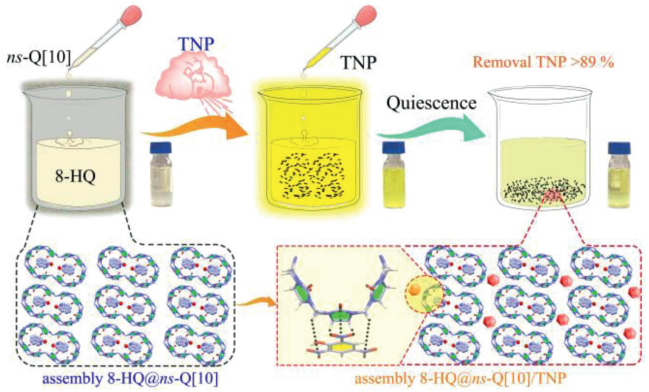

Scheme 1. Schematic diagram of the supramolecular assembly 8-HQ@*ns*-Q[10] for the detection and removal of TNP.

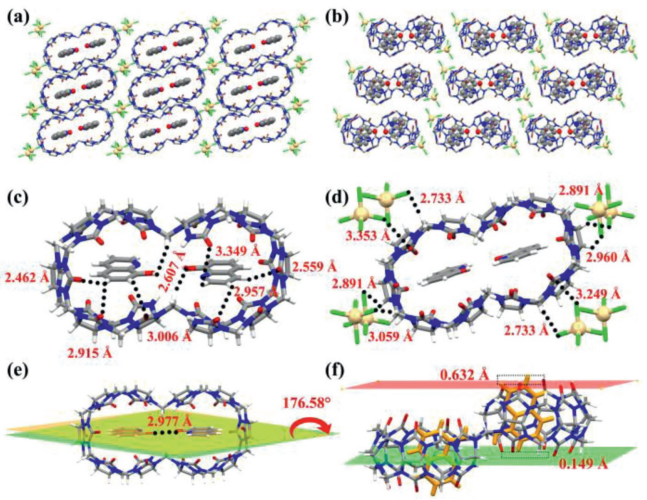

Fig. 1. (a, b) Two-dimensional network of supramolecular organic framework 8-HQ@*ns*-Q[10]/Cd; (c) Intermolecular hydrogen bonding between *ns*-Q[10] host and two 8-HQ molecules; (d) Ion dipole interaction between *ns*-Q[10] host and its surrounding eight $[CdCl_4]^{2-}$; (e) Two 8-HQ molecules were encapsulated in the *ns*-Q[10] host to form near-co-planar structure; (f) The spatial arrangement structure of *ns*-Q[10] host and two 8-HQ molecules in the vertical direction.

organic framework materials that have been reported for the detection of TNP, most of them are fluorescence quenching detection mechanisms. Therefore, the development of a fluorescence-enhanced organic framework material for efficient and rapid detection of TNP is an important part of the current research. Herein, we report cucurbit[*n*]uril as a raw material for constructing supramolecular assembly materials and successfully applied it to fluorescence sensing of TNP.

Cucurbit[*n*]urils (Q[*n*] or CB[*n*]), a family of pumpkin shaped macrocycle host molecules, have specific and strong binding affinities to various guest molecules, which has developed immensely over the past few decades on account of their high selectivity and exceptionally high binding constants in water [22–35]. In 2006, Isaacs reported the synthesis and isolation of *nor-seco*-cucurbit[10]uril (*ns*-Q[10]), which is a double cavity host molecule, each shaped by five glycolurils and connected by two CH_2−bridge [36]. Two cavities of *ns*-Q[10] are able to simultaneously encapsulate two guest molecules to form 1:2 ternary complexes [37]. To date, *ns*-Q[10] have been employed in a variety of applications including molecular recognition [38,39], supramolecular polymers [40,41], supramolecular hydrogel [42], host-guest complexes [43–45], supramolecular organic framework [46], and adsorption separation materials [47]. However, its application as a supramolecular assembly for the preparation of chemical sensors are rarely reported yet.

In this paper, we use *ns*-Q[10] as the host molecule, which mediates two 8-hydroxyquinoline (8-HQ) molecules to form ternary supramolecular assembly. The X-ray single crystal structure shows that the supramolecular assembly 8-HQ@*ns*-Q[10] is mainly formed by *ns*-Q[10] and 8-HQ through numerous intermolecular hydrogen bonds. In addition, 8-HQ is arranged in a top-top conformation in the cavity of *ns*-Q[10], and the two 8-HQ molecules distributed in the two cavities are arranged parallel to each other through intermolecular hydrogen bonds, which result that the rotation of 8-HQ in the cavity is greatly suppressed, and an extremely stable supramolecular assembly 8-HQ@*ns*-Q[10] is formed. Subsequently, the assembly 8-HQ@*ns*-[10] was used for the detection of TNP, and the fluorescence intensity of 8-HQ@*ns*-[10] increased continuously with the addition of TNP (with 27-fold enhancement), with a detection limit of 2.07×10^{-5} mol/L, which also can achieve effectively removing TNP from the aqueous solution (Scheme 1). Thus, this supramolecular assembly 8-HQ@*ns*-Q[10] provides a simple and convenient strategy for the detection and removal of TNP in aqueous environment for future research.

Herein, we constructed a supramolecular assembly 8-HQ@*ns*-Q[10], that is, two 8-HQ molecules were mediated by *ns*-Q[10] to form a ternary host-guest complex, which was induced by the $[CdCl_4]^{2-}$ anions and slowly evaporated in aqueous hydrochloric acid solution, and successfully obtained bright yellow massive single crystal particles, then the structure was characterized by using single crystal X-ray diffraction (Fig. 1 and Table S1 in Supporting information). Single crystal X-ray diffraction analysis showed that supramolecular assembly 8-HQ@*ns*-Q[10] crystallized in the triclinic crystal system with space group *P-1*. The asymmetric unit of supramolecular assembly 8-HQ@*ns*-Q[10] contains an *ns*-Q[10] macrocyclic host, two 8-HQ guest molecules, two tetrahedral $[CdCl_4]^{2-}$ anions, and four protonated water molecules. As shown in Figs. 1a and b, two 8-HQ molecules were encapsulated in the *ns*-Q[10] host and formed a homologous ternary inclusion complex 8-HQ@*ns*-Q[10], the hydrogen atoms on the benzene unit and pyridine unit of the 8-HQ molecule are located at the negatively charged ports of *ns*-Q[10], respectively. Furthermore, in the assembly 8-HQ@*ns*-Q[10], the farthest distances from the hydrogen atom on the pyridine unit and benzene unit of 8-HQ molecule escaping from the *ns*-Q[10] portal plane are 0.632 Å and 0.149 Å, respectively (Fig. 1f). Such a small distance indicates that the size of 8-HQ molecule is almost perfectly consistent with the cavity height of *ns*-Q[10]. The hydrogen atom of the 8-HQ molecule forms a hydrogen bond with the carbonyl oxygen atom of the *ns*-Q[10] host, and the C–H···O distance is 2.462–3.349 Å (Fig. 1c), the hydroxyl groups of two 8-HQ molecules distributed in different cavities of *ns*-Q[10] can form intermolecular hydrogen bonds, and the distance of H–O···H is 2.977 Å (Fig. 1e). Interestingly, the two 8-HQ molecules undergo a reverse subparallel arrangement with a face angle of 176.58° (Fig. 1e). An important reason for such a parallel arrangement is the multiple non-covalent interactions between the 8-HQ guest molecule and the *ns*-Q[10] host. Another important reason is the hydrogen bonding interaction between the hydroxyl groups of two 8-HQ molecules, which further restricts the rotation of 8-HQ molecules in the *ns*-Q[10] host cavity (Fig. 1e). The sophisticated and abundant intermolecular hydrogen bonding resulted in the regular arrangement of 8-HQ within the *ns*-Q[10] host cavity, forming the supramolecular assembly 8-HQ@*ns*-Q[10].

Next, the extended structure of supramolecular assembly 8-HQ@*ns*-Q[10] was analyzed. Since $[CdCl_4]^{2-}$ anions was doped as an inducing reagent during the crystallization process, which also played an important role in the assembly process of the assembly 8-HQ@*ns*-Q[10]. Each 8-HQ@*ns*-Q[10] unit is surrounded by four

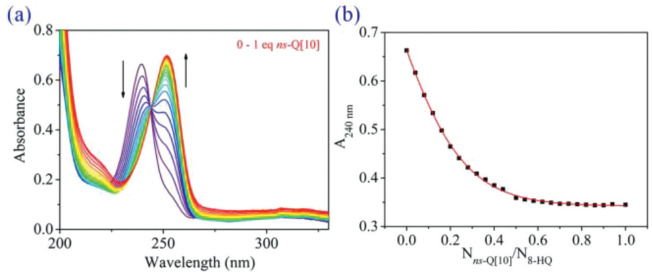

Fig. 2. (a) UV–vis spectral changes of 8-HQ upon addition of *ns*-Q[10] in aqueous solution at 298 K ([8-HQ] = 2.0 × 10^{-5} mol/L and [*ns*-Q[10]] = 0–2.0 × 10^{-5} mol/L). (b) The UV–vis spectral changes *versus* the molecular ratio of *ns*-Q[10]/8-HQ.

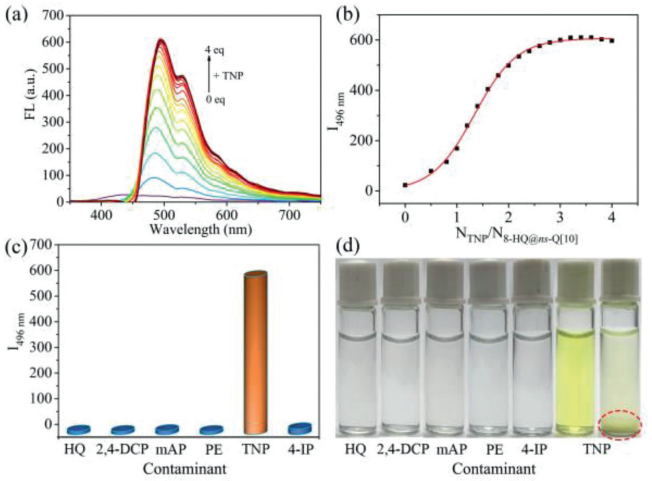

Fig. 3. (a) Fluorescence spectra obtained for 8-HQ@*ns*-Q[10] (2.0 × 10^{-5} mol/L) upon increasing the concentration of TNP in water (λ_{ex} = 240 nm). (b) Change in fluorescence intensity with $N_{[TNP]}/N_{[8-HQ@ns-Q[10]]}$, (c) fluorescence response ability of 8-HQ@*ns*-Q[10] (2.0 × 10^{-5} mol/L) to some analogues of TNP (HQ, 2,4-DCP, mAP, PE, 4-IP, 4.0 × 10^{-5} mol/L); (d) Photographs of 8-HQ@*ns*-Q[10] (2.0 × 10^{-5} mol/L) on addition of HQ, 2,4-DCP, mAP, PE, 4-IP and TNP from left to right, respectively, and let stand for 30 min.

repeating units and eight tetrahedral $[CdCl_4]^{2-}$ anions (Fig. 1c, Figs. S1a and b in Supporting information), each $[CdCl_4]^{2-}$ anions forms C–H···Cl contact with adjacent *ns*-Q[10] hosts with a C–H···Cl distance of 2.733–3.353 Å The C–H bonds of the methyl or methylene groups on the outer surface of the *ns*-Q[10] host interact with the carbonyl oxygens of the adjacent *ns*-Q[10] host to form abundant C–H···O hydrogen bonds, C–H···O distances with 2.573–3.192 Å (Figs. S1c and d in Supporting information). Both C–H···Cl interactions and C–H···O hydrogen bonds contribute to stabilize the structure of the supramolecular assembly 8-HQ@*ns*-Q[10], and these are classified as "outer surface interaction of cucurbit[*n*]urils" [48–53].

A detailed analysis of the crystal structure of the supramolecular assembly 8-HQ@*ns*-Q[10] showed that it does perform regular assembly in the solid state and the stoichiometric ratio of *ns*-Q[10] to 8-HQ is 1:2. Further, we investigated whether it can also be efficiently assembled in the liquid dispersion state by UV–vis spectroscopy and ^{1}H NMR. Firstly, the host-guest interaction between *ns*-Q[10] and 8-HQ was investigated by UV–vis spectroscopy, as Fig. 2 shows, in the initial state, 8-HQ had an adsorption peak (λ=240 nm) in aqueous solution. With the gradual addition of *ns*-Q[10], the adsorption peak at 240 nm decreased gradually, accompanied by a red shift of 12 nm, and the adsorption peak at 252 nm increased at the same time (Fig. 2a), Job's plots and mole ratio method of 8-HQ and *ns*-Q[10] measured by UV–vis absorption spectrum prove that the stoichiometric ratio of *ns*-Q[10] and 8-HQ is 1:2 (Fig. 2b and Fig. S2 in Supporting information). Then the ^{1}H NMR spectrum was used to further analyze its binding mode (Fig. S3 in Supporting information), when the guest is encapsulated in the cavity of *ns*-Q[10], the proton signal of the guest will shift to the upfield. In contrast, the portal of *ns*-Q[10] is a proton deshielding region. Therefore, it is convenient to infer the binding pattern of the *ns*-Q[10] host to 8-HQ from the changes by their ^{1}H NMR spectra. In the process of ^{1}H NMR titration, the amount of *ns*-Q[10] (1.0 × 10^{-4} mol/L, D_2O) was fixed to continuously increase the content of 8-HQ in the system, which show that proton signal peaks $H_{a\text{-}b}$ undergo downfield shift (ΔH_a= 0.11 ppm, ΔH_b= 1.12 ppm), and proton signal peaks $H_{c\text{-}f}$ are shifted upfield (ΔH_c= 0.55 ppm, ΔH_d= 0.26 ppm, ΔH_e= 0.29 ppm, ΔH_f= 0.18 ppm). When the stoichiometric ratio of *ns*-Q[10] to 8-HQ is 1:2, the system reaches the equilibrium state. Meanwhile, only the edge hydrogen atoms (H_a and H_b) of the benzene unit of the 8-HQ molecule are located on the port of *ns*-Q[10], and all the remaining benzene ring units are located inside the cavity of *ns*-Q[10]. This is in perfect agreement with the structure of the assembly 8-HQ@*ns*-Q[10] in the crystalline state. It can be concluded that both in the liquid state and in the solid state, *ns*-Q[10] and 8-HQ are able to form a stable assembly 8-HQ@*ns*-Q[10], and the stoichiometric ratio of *ns*-Q[10] to 8-HQ is 1:2.

Based on the above experimental results, we applied the supramolecular assembly 8-HQ@*ns*-Q[10] with good water solubility and stable structure to selectively detect and remove TNP. It was found that 8-HQ@*ns*-Q[10] shows almost fluorescence silent in the aqueous, and when a certain amount of TNP was added to the assembly 8-HQ@*ns*-Q[10] system, the fluorescence intensity of the system was increased (Fig. 3a). Fig. 3b shows the change trend of fluorescence intensity after adding TNP into the assembly, and the molar ratio of TNP to 8-HQ@*ns*-Q[10] after interaction reaches equilibrium. Specifically speaking, the fluorescence intensity was enhanced from 22 to 600 with the gradual addition of TNP to the assembly 8-HQ@*ns*-Q[10] system (0.0–4.0 equiv.), with a 27-fold fluorescence enhancement (λem = 496 nm). As a contrast, without *ns*-Q[10], this fluorescent enhanced detection cannot occur, which also proves the important role of the assembly 8-HQ@*ns*-Q[10] (Fig. S4 in Supporting information). Meanwhile, with the continuous addition of TNP into the assembly 8-HQ@*ns*-Q[10] aqueous solution, its UV–vis absorption spectrum also showed regular changes, with the UV–vis absorption peak at 240 nm continuously enhanced, accompanied by a new absorption peak at 356 nm (Fig. S5 in Supporting information). This indicates that the assembly 8-HQ@*ns*-Q[10] can serve as a potential candidate for sensing TNP in water. The detection limit of 8-HQ@*ns*-Q[10] to TNP was 2.07 × 10^{-5} mol/L (Fig. S6 in Supporting information), in addition, the assembly 8-HQ@*ns*-Q[10] has no significant fluorescence response ability to other phenolic pollutants (hydroquinone: HQ; 2,4-dichlorophenol: 2,4-DCP; *m*-aminophenol: *m*-AP; phenol: PE; 4-(imidazol-1-yl)phenol: 4-IP, Fig. 3c), and the detection process is almost undisturbed when multiple pollutants coexist, which proves that the detection of assembly 8-HQ@*ns*-Q[10] to TNP has good specificity and anti-interference ability.

To investigate the sensing mechanisms of 8-HQ@*ns*-Q[10] to TNP, the normalized absorption of TNP and emission spectra of assembly 8-HQ@*ns*-Q[10] and 8-HQ@*ns*-Q[10]/TNP were measured, which turns out that it's a FRET processes. As shown in Fig. S7 (Supporting information), a good overlap between the absorption spectrum of TNP and the emission spectrum of assembly 8-HQ@*ns*-Q[10] was clearly observed. Subsequently, the FRET process from assembly 8-HQ@*ns*-Q[10] to TNP was monitored. With the gradual addition of TNP into the 8-HQ@*ns*-Q[10] solution, the emission intensity of 8-HQ@*ns*-Q[10] at 438 nm exhibited a dramatic decrease accompanied by an obvious increase at 496 nm when excited at 240 nm (Fig. 3a). The observed phenomena were consistent with

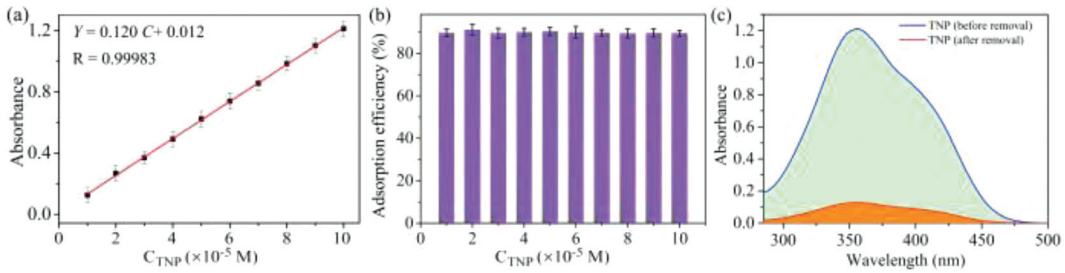

Fig. 4. (a) UV–vis absorption standard curve of TNP; (b) Histogram of absorption efficiency of assembly 8-HQ@*ns*-Q[10] (2.0×10^{-5} mol/L) to TNP with different concentrations (10^{-6}–10^{-4} mol/L); (c) The UV–vis absorption spectrum of liquid phase with 10^{-4} mol/L TNP (before and after adsorption).

the typical FRET process in which the assembly 8-HQ@*ns*-Q[10] acted as the donor and the TNP acted as the acceptor. This process is also accompanied by a greatly enhanced fluorescence of the system.

Interestingly, 8-HQ@*ns*-Q[10] not only specifically recognizes TNP, but also effectively removes the residual TNP from aqueous solutions. 8-HQ@*ns*-Q[10] was gradually added to the TNP solution and left to stand for about 30 min, then a large amount of precipitate appeared at the bottom of the solution (Fig. 3d), which could be separated by high-speed centrifugation. Subsequently, the liquid phase were subjected to UV–vis spectroscopy, and the standard curve of TNP was plotted ($y = 0.120$ C + 0.012, $R = 0.99983$, Fig. 4a). Based on Lambert's law, the residual amount of TNP in water was calculated to be 10.63 μmol/L when the initial concentration of TNP is 100.07 μmol/L, and the average removal rate is 89.83% (Figs. 4b and c, Table S2 in Supporting information), which indicates that 8-HQ@*ns*-Q[10] can effectively remove TNP from water. Moreover, the precipitate was measured by Fourier Transform infrared spectroscopy (FTIR) (Fig. S8 in Supporting information), the characteristic bands of TNP and assembly 8-HQ@*ns*-Q[10] can be observed in the FTIR spectrum of the precipitated product. The O–H stretching vibration appearing at 3433 cm^{-1}, which can be attributed to the carboxyl moiety of 8-HQ. The band at 1730 cm^{-1} arises from the C=O stretching vibration of *ns*-Q[10]. The bending vibration of methylene of *ns*-Q[10] appears at 1470 cm^{-1}, the C–C stretching vibration and the deformation vibrations of the glycoluril ring appears at 967 cm^{-1} and 803 cm^{-1}, respectively. A wider band appeared at 1229 cm^{-1} belonging to the C–O stretching vibration of TNP. Therefore, it can be said that the precipitate is a 8-HQ@*ns*-Q[10]/TNP complex.

Further experimental studies were carried out to investigate the removal mechanism of the assembly 8-HQ@*ns*-Q[10] to TNP. With the continuous addition of TNP to the assembly 8-HQ@*ns*-Q[10], the ^{1}H NMR signal peak of 8-HQ is obviously weakened, gradually blunted until disappearing, accompanied by a slight shift to the downfield. Meanwhile, the signal peak of TNP became more and more sharp and obvious, and did not shift and the signal peak of *ns*-Q[10] did not shift and decrease from the beginning to the end (Fig. 5 bottom). Furthermore, the solution changes from a colorless clarified solution to a yellow suspension until a large amount of yellow precipitate is produced (Fig. 5 top). As a comparison, the interaction between TNP and *ns*-Q[10], as well as the interaction between TNP and 8-HQ was also investigated, respectively. The results show that the mixture of *ns*-Q[10] and TNP can precipitate rapidly (Fig. S9 in Supporting information), while the mixture of 8-HQ and TNP are always in solution state (Fig. S10 in Supporting information). Based on the above experimental phenomena, since the electropositive outer surface of *ns*-Q[10] possesses an inherent affinity toward the electron negative TNP, we speculate that TNP molecule contains aromatic ring, nitro group and hydroxyl group, which is easy to form multiple non-covalent interactions with the outer surface of *ns*-Q[10], these interactions between *ns*-Q[10] and

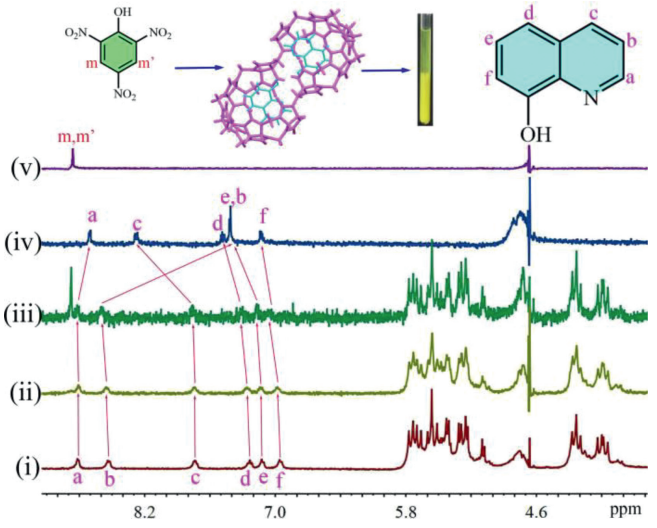

Fig. 5. (Top) the 8-HQ@*ns*-Q[10] solution changes in color and state after added TNP, (bottom) ^{1}H NMR titration spectra (400 MHz, D_2O, 298 K) of 8-HQ@*ns*-Q[10] (1.0×10^{-4} mol/L) in the presence of TNP, (i) 0, (ii) 1.0, (iii) 2.0 equiv of TNP, (iv) free 8-HQ and (v) free TNP.

TNP makes the formed complex precipitate out of solution, so as to achieve an efficient removal of TNP.

In summary, we have successfully constructed a supramolecular assembly 8-HQ@*ns*-Q[10], which has good water solubility and stability. Detailed analysis of its solid-state structure by X-ray single-crystal diffraction. We also proved that its solid-state structure remains highly consistent with the assembly under liquid conditions. Due to the special double cavity structure of *ns*-Q[10], the stoichiometric ratio between *ns*-Q[10] and 8-HQ molecules in this assembly 8-HQ@*ns*-Q[10] is 1:2. The luminescence sensing experiments showed that assembly 8-HQ@*ns*-Q[10] can be applied as a good luminescence sensing material for the detection of pollutants and explosives TNP. The addition of TNP resulted in a rapid increase in the fluorescence of the assembly 8-HQ@*ns*-Q[10], and the fluorescence response with a detection limit of 2.07×10^{-5} mol/L. The mechanism of action of assembly 8-HQ@*ns*-Q[10] to TNP is attributed to FRET process, and the supramolecular assembly 8-HQ@*ns*-Q[10] acts a donor, and TNP act as an acceptor. Furthermore, the collective aggregation precipitation of 8-HQ@*ns*-Q[10]-TNP is triggered by the outer surface interaction with *ns*-Q[10], so as to achieve effectively removing TNP from the water, and removal efficiency is greater than 89%. From the perspective of experimentation and practice, the current work still has certain challenges and practicability. We will continue to construct luminescent assembly based on double-cavity *ns*-Q[10] and explore its application in environmental pollutant detection, we are conducting in-depth excavations and innovative research in this field.

Declaration of competing interest

The authors declare that they have no known competing financial interests or personal relationships that could have appeared to influence the work reported in this paper.

Acknowledgments

We acknowledge the support of the Natural Science Foundation of the Science and Technology Department of Guizhou Province (No. ZK-2021–024), the National Natural Science Foundation of China (No. 22061009) and the Innovation Program for High-level Talents of Guizhou Province (No. 2016–5657).

Supplementary materials

Supplementary material associated with this article can be found, in the online version, at doi:10.1016/j.cclet.2023.108195.

References

[1] K.S. Asha, G.S. Vaisakhan, S. Mandal, Nanoscale 8 (2016) 11782–11786.
[2] P.B. Zhu, L.X. Lin, W. Chen, L. Liu, Chemosphere 302 (2022) 134785.
[3] P.D. Jawale Patil, R.D. Ingle, S.M. Wagalgave, et al., Chemosensors 7 (2019) 38.
[4] M.S. Bishwas, M. Malik, P. Poddar, New J. Chem. 45 (2021) 7145–7153.
[5] S.K. Dinda, M.A. Hussain, A. Upadhyay, C.P. Rao, ACS Omega 4 (2019) 17060–17071.
[6] Y.L. Li, L.Y. Feng, W. Yan, et al., Nanoscale 11 (2019) 1286–1294.
[7] H.P. Wang, L. Zhang, X.Q. Guo, et al., Anal. Chim. Acta 1091 (2019) 76–87.
[8] J.K. Rajput Jigyasa, Sens. Actuators B 259 (2018) 990–1005.
[9] S.M. Tawfik, M. Sharipov, S. Kakhkhorov, M.R. Elmasry, Y. Lee, Adv. Sci. 23 (2019) 1801467.
[10] W.Y. Fang, W. Zhao, P. Pei, et al., J. Mater. Chem. C 6 (2018) 9269–9276.
[11] S. Gai, R.Q. Fan, J. Zhang, et al., Inorg. Chem. 60 (2021) 10387–10397.
[12] L. Esrafili, M. Gharib, A. Morsali, P. Retailleau, Ultrason. Sonochem. 66 (2020) 105110.
[13] S.S. Dhankhar, N. Sharma, S. Kumar, T.J.D. Kumar, C.M. Nagaraja, Chem. Eur. J. 23 (2017) 16204–16212.
[14] X.M. Zhang, Z.M. Gou, Y.J. Zuo, W.Y. Lin, J. Photochem. Photobiol. A 401 (2021) 113183.
[15] S. Saravanan, R. Ahmad, S. Kasthuri, et al., Mater. Chem. Front. 5 (2021) 238–248.
[16] S.F. Xu, H.Z. Lu, J.H. Li, et al., ACS Appl. Mater. Interfaces 5 (2013) 8146–8154.
[17] T. Das, M. Mohar, A. Bag, Colloid Interface Sci. Commun. 45 (2021) 100534.
[18] W.F. Xu, H.H. Chen, Z.Q. Xia, et al., Inorg. Chem. 58 (2019) 8198–8207.
[19] G. Radha, T. Leelasree, D. Muthukumar, R.S. Pillai, H. Aggarwal, New J. Chem. 45 (2021) 12931–12937.
[20] F. Afshariazar, A. Morsali, J. Mater. Chem. C 9 (2021) 12849–12858.
[21] M.W. Zhu, S.Q. Xu, X.Z. Wang, et al., Chem. Commun. 54 (2018) 2308–2311.
[22] H.G. Nie, Z. Wei, X.L. Ni, Y. Liu, Chem. Rev. 122 (9) (2022) 9032–9077.
[23] D. Yang, M. Liu, X. Xiao, Z. Tao, C. Redshaw, Coord. Chem. Rev. 434 (2021) 213733.
[24] P.H. Shan, J.H. Hu, M. Liu, et al., Coord. Chem. Rev. 467 (2022) 214580.
[25] R. Cen, M. Liu, H. Xiao, et al., Sens. Actuators B 378 (2023) 133126.
[26] C. Liu, Y. Xia, Z. Tao, X.L. Ni, Chin. Chem. Lett. 33 (2022) 1529–1532.
[27] X.W. Cui, W.X. Zhao, K. Chen, et al., Chem. Eur. J. 23 (2017) 2759–2763.
[28] M. Liu, L.X. Chen, P.H. Shan, et al., ACS Appl. Mater. Inter. 13 (2021) 7434–7442.
[29] M. Liu, R. Cen, J. Zhao, et al., Sep. Purif. Technol. 304 (2023) 122342.
[30] M. Liu, J.L. Kan, Y.Q. Yao, Sens. Actuators B 283 (2019) 290–297.
[31] M. Liu, M.X. Yang, Y.Q. Yao, et al., J. Mater. Chem. C 7 (2019) 1597–1603.
[32] H.G. Nie, Y.T. Rao, J.X. Song, X.L. Ni, Chem. Mater. 34 (2022) 8925–8934.
[33] H.Q. Shen, C. Liu, J. Zheng, et al., ACS Appl. Mater. Interfaces 13 (2021) 55463–55469.
[34] M. Peng, Y. Luo, Y.T. Rao, J.X. Song, X.L. Ni, Chem. Eur. J. 28 (2022) e202202056.
[35] C. Sun, Z.Y. Wang, L.D. Yue, et al., J. Am. Chem. Soc. 142 (2020) 16523–16527.
[36] W.H. Huang, S.M. Liu, P.Y. Zavalij, L. Isaacs, J. Am. Chem. Soc. 128 (2006) 14744–14745.
[37] J.B. Wittenberg, M.G. Costales, P.Y. Zavalij, L. Isaacs, Chem. Commun. 47 (2011) 9420–9422.
[38] D. Lucas, T. Minami, G. Iannuzzi, et al., J. Am. Chem. Soc. 133 (2011) 17966–17976.
[39] L. Isaacs, Acc. Chem. Res. 47 (2014) 2052–2062.
[40] E.A. Appel, J.D. Barrio, J. Dyson, L. Isaacsb, O.A. Scherman, Chem. Sci. 3 (2012) 2278–2281.
[41] Y.C. Yang, X.L. Ni, J.F. Xu, X. Zhang, Chem. Commun. 55 (2019) 13836–13839.
[42] K.M. Park, J.H. Roh, G. Sung, J. Murray, K. Kim, Chem. Asian J. 12 (2017) 1461–1464.
[43] X.D. Zhang, W. Wu, Z. Tao, X.L. Ni, Beilstein J. Org. Chem. 15 (2019) 1705–1711.
[44] G. Carroy, V. Lemaur, J.D. Winter, et al., Phys. Chem. Chem. Phys. 18 (2016) 12557–12568.
[45] M.I. El-Barghouthi, H.M. Abdel-Halim, F.J. Haj-Ibrahim, K. Bodoor, K.I. Assaf, J. Incl. Phenom. Macrocycl. Chem. 82 (2015) 323–333.
[46] P.Q. Zhang, Q. Li, Z.K. Wang, et al., Chin. Chem. Lett. 34 (2023) 107632.
[47] M. Liu, R. Cen, J.S. Li, et al., Angew. Chem. Int. Ed. 61 (2022) e202207209.
[48] L.F. Tian, M. Liu, L.X. Chen, et al., Chin. Chem. Lett. 33 (2022) 1524–1528.
[49] Y. Huang, R.H. Gao, M. Liu, et al., Angew. Chem. Int. Ed. 60 (2021) 15166–15191.
[50] M. Liu, Y. Zhou, L.X. Chen, et al., Chin. Chem. Lett. 32 (2021) 375–379.
[51] C. Liu, R.H. Gao, Y.Q. Zhang, Q.J. Zhu, Z. Tao, Chin. Chem. Lett. 32 (2021) 362–366.
[52] L.X. Chen, M. Liu, Y.Q. Zhang, et al., Chem. Commun. 55 (2019) 14271–14274.
[53] Y.Q. Yao, Y.J. Zhang, Y.Q. Zhang, et al., ACS Appl. Mater. Interfaces 9 (2017) 40760–40765.